Internal seiches in a karstic mesotrophic lake (Prošće, Plitvice Lakes, Croatia)

Zvjezdana B. Klaić [1], Karmen Babić [1,2] and Tomislav Mareković [3]

[1] Department of Geophysics, Faculty of Science, University of Zagreb,
Horvatovac 95, 10000 Zagreb, Croatia

[2] Croatia Control Ltd., Velika Gorica, Croatia

[3] Croatian Meteorological and Hydrological Service, Zagreb, Croatia

A lake temperature experiment was performed at the Prošće, Plitvice Lakes, Croatia during a 4-month observational period (6 July–4 November, 2019) to investigate the occurrence and characteristics of internal seiches in the lake. Two-minute mean lake temperatures were measured at a single lake point at fifteen depths ranging from 0.2 to 27 m. Analysis of these data provided insight into the previously unknown and rather complex Prošće Lake seiching. Power spectral densities (PSDs) and magnitude-squared coherences (γ^2), together with corresponding cross-spectrum phases that were obtained from the hourly mean lake temperature, air pressure and wind speed data, suggested the presence of three vertical modes of an internal seiche. The first mode (V1H1, period of 6.09 h) corresponds to free baroclinic oscillations; the second mode (V2H1, period of 11.64 h) and the third mode (V3H1, period of 25.60 h) are associated with forced baroclinic oscillations of the lake interior. Excitation of the higher vertical modes is attributed to the influence of dense tributary water. Due to this water influence, vertical temperature gradients in the lake interior were relatively weak; consequently, a single thick metalimnion and/or two metalimnetic layers were established, which resulted in the presence of the V2H1 and V3H1 modes, respectively. Additionally, due to the influence of tributary water, the lake did not attain the typical stratification that is characterized by hypolimnetic temperatures of ≈ 4°C. Instead, during the entire observational period, the hypolimnetic temperatures were consistently above 7.6 °C.

Keywords: coherence, higher vertical modes, internal seiche, power spectral density, V2H1, V3H1

1. Introduction

Prošće Lake is the second largest out of sixteen karstic Plitvice Lakes. The lakes are located in a mountainous region of Croatia and are part of Plitvice Lake National Park (hereafter, PLNP). The lakes form an approximately 9 km long chain that extends in

roughly a south-north direction and the lakes are interconnected by waterfalls and cascades. The southernmost lake, Prošće Lake (Fig. 1), is the first in the lake system. It also is oriented in approximately the south-north direction. Prošće Lake is mainly fed by the Matica River, and to a lesser extent by Sušanj Stream. Matica River is formed by the confluence of two springs, *Bijela rijeka* and *Crna Rijeka* and it is 76 ± 8 cm deep (Vurnek et al., 2016). The lake altitude, area, maximum depth and volume are 636.6 m, 682,000 m², 37.4 m and $7.67 \cdot 10^6$ m³, respectively (*e.g.*, Babinka, 2007). The maximum lake fetch is approximately 2 km, while its greatest width (perpendicular to the lake's north-south axis) is approximately 430 m. While the remaining fifteen lakes are oligotrophic, Prošće Lake is mesotrophic (Petrik, 1961). Thus, a comparison of the optical properties of the
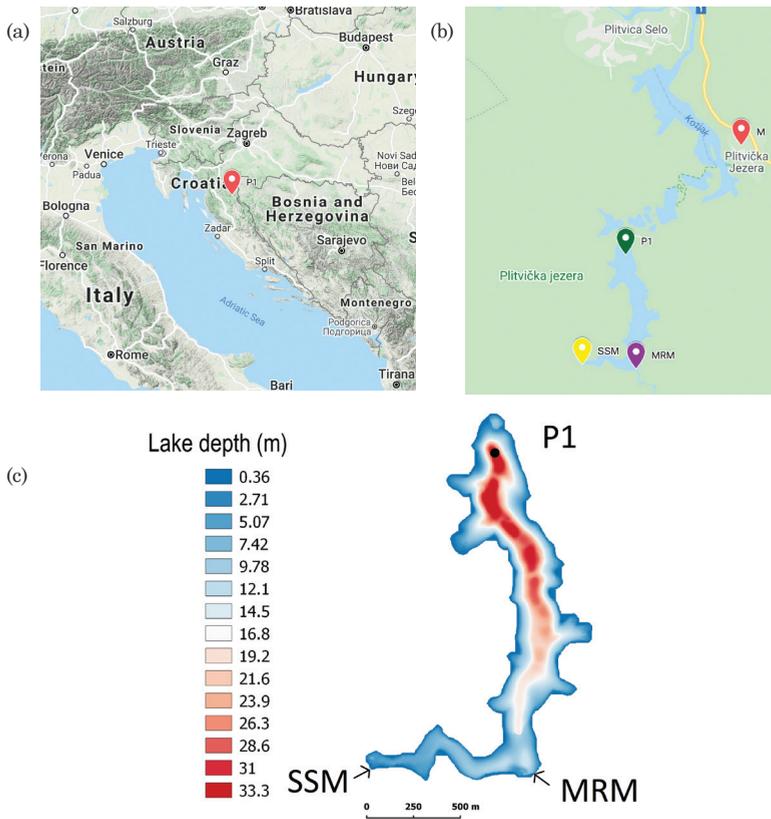
Figure 1. Position of Prošće Lake (red bubble, panel *a*). A closer look at the first twelve lakes. Green and red bubbles correspond to the positions of the lake temperature measuring point P1 ($\varphi = 44.8676°$ N, $\lambda = 15.5981°$ E) and a meteorological measuring site M ($\varphi = 44.8811°$ N, $\lambda = 15.6197°$ E, 579 m ASL) that is approximately 2 km away. Positions of Matica River (MRM) and Sušanj Stream (SSM) mouths are indicated by violet and yellow bubles, respectively (*b*). The most recent bathymetry of Prošće Lake was determined in 2019 and was provided by PLNP. Positions of point P1 and stream mouths (MRM and SSM) are indicated by the black circle and black arrows, respectively (*c*). (Source of panels *a* and *b*: © Google Maps).

three largest lakes, namely, Prošće, Galovac and Kozjak (1st, 8th and 12th lakes in the chain, respectively) showed that among these three lakes, Prošće had the highest turbidity (Golubić, 1966). In recent decades, intensification of the eutrophication process of Prošće Lake has been observed, as was described in a sediment composition study by Horvatinčić et al. (2018).

A recent review of studies addressing the abiotic properties and processes in Plitvice Lakes (Klaić et al., 2018) pointed to a lack of investigations in the field of physical limnology (this is also valid for other Croatian lakes). Thus far, when considering physical topics, only barotropic, surface seiches (Gavazzi, 1919; Pasarić and Slaviček, 2016) for the two largest lakes, Prošće and Kozjak (1st and 12th in the lake chain, respectively) and baroclinic, internal seiches in Kozjak (Klaić et al., 2020) have been studied. In comparison with surface seiches, internal seiches (*e.g.*, Mortimer, 1953; Heaps, 1961; Münnich et al., 1992; Fricker and Nepf, 2000) are far more important for lakes as the restoring forces (which strive to restore equilibrium at the surface between the two distinct layers) are generally proportional to the density difference between the two layers. Accordingly, for the case of surface seiches, the restoring forces are strong (since they are proportional to the high density difference between the air and lake water) while for internal seiches they are much weaker (they are proportional to the much smaller density difference between epilimnetic and hypolimnetic waters). Consequently, internal seiches have higher amplitudes and longer periods than surface seiches and can result in mixing and redistribution of water and nutrients within a lake and in energy transfer. Due to periodic vertical displacements of the suspended biomass, internal seiches can also affect the intensity of the light that is available to algae and phytoplankton (*e.g.*, Paul, 1987; Pannard et al., 2011).

The simplest case of an internal seiche is one that has only one vertical and one horizontal mode (V1H1). It occurs if the thickness of metalimnion (thermocline region) is constant over time (*e.g.*, Münnich et al., 1992, Vidal et al., 2005; Pannard et al., 2011). For that case, only one nodal point in the horizontal and one in the vertical direction are found and a two-layer model with the epilimnion and hypolimnion as the distinct layers can be assumed. However, if more lake layers are present, higher vertical modes may occur. The second vertical first horizontal mode (V2H1) is associated with a change of metalimnion thickness and consequent oscillations in the hypolimnion and epilimnion which oscillate against each other. For that case, two nodal points are present in the vertical direction while there is one nodal point in the horizontal direction. Thus, for that case, a three-layer model can be assumed. The presence of more lake layers (*i.e.*, multiple metalimnetic layers) can lead to even higher vertical modes such as V3H1 (with three nodal points in the vertical direction and one in the horizontal direction) and V4H1 (four nodal points in the vertical direction and one in the horizontal direction), which correspond to four and five lake layers, respectively. In such cases, each pair of two neighboring layers oscilate against each other. Of course, higher horizontal modes are also possible, as well as any combination of *i* and *j* (that is, V*i*H*j*) for which *i* and *j* correspond to the number of nodal points in the vertical and horizontal directions, respectively. A sketch of V1H1, V2H1 and V3H1 modes is shown in Appendix.

In lakes and reservoirs, the most commonly observed mode is the V1H1 mode (*e.g.*, Vidal et al., 2007; Simpson et al., 2011); however, the presence of higher vertical modes has also been reported (*e.g.*, Münnich et al., 1992; Vidal et al., 2005, 2007, 2008; Pannard et al., 2011; Simpson et al., 2011; Valerio et al., 2019), and it is even possible to reach the 5th mode V5 (Vidal et al., 2007).

With an aim of acquiring further knowledge on the physics of Plitvice Lakes, in the present study we focus on the internal seiches in Prošće Lake. Based on experimental data of lake temperatures, we will show that the seiching in Prošće Lake is rather complex and that apart from the first mode, higher vertical modes are also excited.

2. Lake temperature and meteorological measurements

2.1. Lake temperatures

Lake temperatures were measured with factory calibrated HOBO TidBit 400 sensors (Onset Computer Corporation, Bourne, USA). These sensors measure temperature every second with accuracy of ±0.20 °C (for the temperature range of 0 to 70 ˚C), and they are equipped with data loggers. The averaging interval of the stored data, which is specified by the user, was here set to 2 min. For the purpose of the present study, fifteen sensors were fastened to a string at depths which ranged from 0.2 to 27 m. To obtain finer vertical resolution of the measured temperatures closer to the lake surface, the sensors were placed at depths of 0.2, 0.5, 1, 1.5, 3, 5, 7, 9, 11, 13, 15, 17, 20, 23, and 27 m. Point P1 is located in the northern, deepest part of the lake (Fig. 1 panels b and c). The string with sensors was attached to a buoy and was moored to ensure a fixed position at point P1 ($\varphi = 44.8676°$ N, $\lambda = 15.5981°$ E). The maximum lake depth at this location was 32.5 m. Two-minute mean lake temperatures were recorded continuously from 6 July, 2019 at 00:00 h local standard time (hereafter LST; without summertime advancement by one hour) to 4 November, 2019 at 00:00 LST.

2.2. Meteorological data

Meteorological data that were concurrent with the lake temperature observations were obtained from the automatic meteorological station Plitvička Jezera (point M in Fig. 1b, $\varphi = 44.8811°$ E, $\lambda = 15.6197°$ E, altitude 579 m ASL). The station is approximately 2 km distant from point P1. Station maintenance and quality control of the measured data are performed by the Croatian Meteorological and Hydrological Service. The available data include hourly mean values of the surface (2 m above ground level) air temperature, UVB radiation, air pressure, atmospheric relative humidity, hourly precipitation amount, and surface (10 m above ground level) wind speed and wind direction.

3. Methods

In addition to the standard statistical procedures, spectral analysis as described in more detail in Klaić et al. (2020) was conducted. Specifically, the power spectral density (PSD) was determined using Welch's method (Welch, 1967) (also known as the weighted overlapped segment averaging (WOSA) method or periodogram averaging method). Here, each input time series was split into eight segments of equal length with 50% overlap. The segments were windowed with a Hamming window (*e.g.*, Patel et al., 2013). The window lengths were set to 512 and 128 data points for analysis of the data that corresponded to the entire observational period (6 July–4 November, 2019) and 30-day time interval which was associated with the predominately along-basin winds (22 September–21 October, 2019), respectively.

Magnitude-squared coherence values between lake temperatures at all lake depths and lake temperatures at particular depths along with the corresponding cross-spectrum phases, which were calculated here for selected time interval associated with predominately along-basin winds, were determined based on the same parameters as those used in the PSD calculations. Specifically, the input time series segments were windowed with a Hamming window with a window length of 128 data points and 50% overlap. In the PSDs, coherence and cross-spectrum phase calculations built-in functions of the MATLAB software (Version R2010b) *pwelch*, *mscohere* and *cpsd* were used, respectively.

Water density ρ (kg m^{-3}) and squared Brunt-Väisälä frequency N^2 (s^{-2}) values were calculated from the following formulas (*e.g.*, Sun et al., 2007):

$$\rho = (1 - 1.9549 \cdot 10^{-5} \, [T - 277]^{1.68}) \cdot 10^3, \tag{1}$$

$$N^2 = (- g / \rho)(\partial \rho / \partial z), \tag{2}$$

where T is the observed water temperature, g is acceleration of gravity ($g = 9.81$ m s^{-2}), and the vertical axis z in the calculation of the term $\partial \rho / \partial z$ is oriented from the lake bottom toward the lake surface.

Generally, the Brunt-Väisälä frequency provides information on the hydrostatic stability of the water column and on the strength of vertical stratification of density where $N^2 > 0$, $N^2 = 0$, and $N^2 < 0$ correspond to hydrostatically stable, neutral and unstable stratification, respectively. Furthermore, N (which is associated with restoring gravity force) corresponds to the maximum possible frequency of an internal wave. Thus, it is one of the key parameters in the theory of internal waves (*e.g.*, Gerkema and Zimmerman, 2008).

Theoretical periods of V1H1 and V2H1 modes were calculated by assuming an idealized, rectangular, elongated lake of constant depth. This idealized lake has homogenous fluid layers and it is exposed to along-basin wind. Further, due to its size, the lake is not affected by the Coriolis force. Under the above assumptions, the period of V1H1 mode can be determined from the Watson's solution for the two-layer model (Watson, 1904):

$$\tau_{11} = 2L / [g(\rho_H - \rho_E) / (\rho_H / h_H + \rho_E / h_E)]^{1/2}, \tag{3}$$

where τ_{11} is the period of V1H1 mode (s), L is the basin length, $g = 9.81$ m s^{-2} is the acceleration due to gravity and ρ_H and ρ_E are the densities (kg m^{-3}) of hypolimnion and epilimnion, while depths of hypolimnion and epilimnion are h_H and h_E (m), respectively.

The period of V2H1 mode was calculated based on the analytical solution of a three-layer model given by Münnich et al. (Münnich et al., 1992; Boegman, 2009; Hutter et al., 2011):

$$\tau_{21} = 2L / [(g / 2h)(\gamma - (\gamma^2 - 4ah)^{1/2})]^{1/2}, \tag{4}$$

where τ_{21} is the period of V2H1 mode (s), h is the total lake depth (m), that is the depth of epilimnion, metalimnion and hypolimnion ($h = h_E + h_M + h_H$). Values of γ and a are determined from following equations:

$$a = h_E h_M h_H (1 - \rho_E / \rho_M)(1 - \rho_M / \rho_H), \tag{5}$$

and

$$\gamma = h_E h_M (1 - \rho_E / \rho_M) + h_E h_H (1 - \rho_E / \rho_H) + h_M h_H (1 - \rho_M / \rho_H), \tag{6}$$

where ρ_M is a density of metalimnion.

4. Results and discussion

Figure 2 shows the lake temperatures at various depths and concurrent meteorological data for the observational period, while Figure 3a shows vertical distribution of lake temperatures. As expected, the air temperature, relative atmospheric humidity, UVB radiation, wind speed and lake temperatures within the first few meters exhibited diurnal variations in the majority of individual days (specifically, for those days with synoptically undisturbed weather conditions). Additionally, we note that the lake temperatures in the bottom layers were always far above the temperature at which a fresh water achieves its maximum density (3.98 °C, Figs. 2b and 3a). During the investigated period,
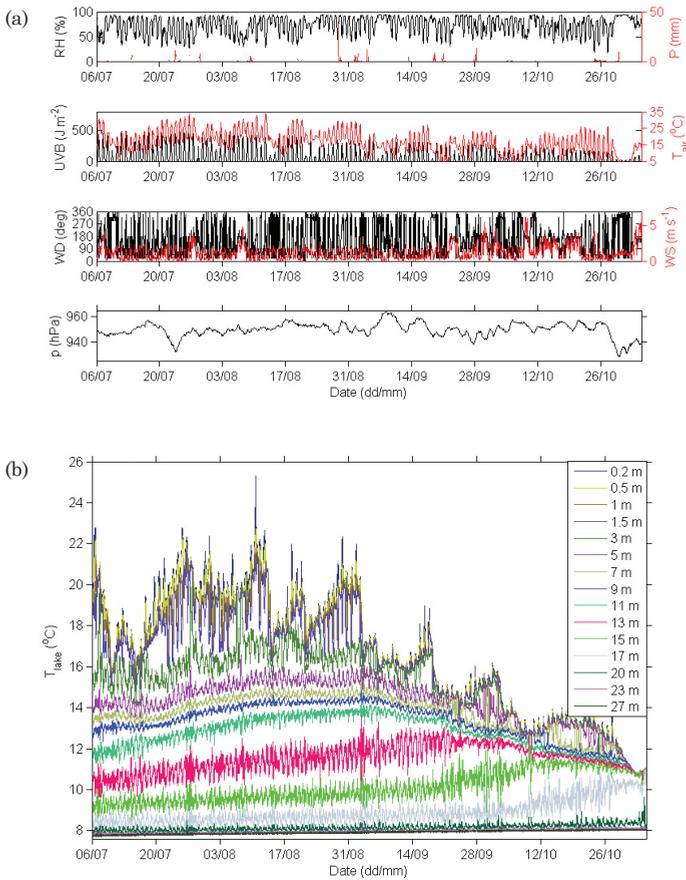
Figure 2. Observed hourly values of meteorological variables: relative atmospheric humidity (*RH*), precipitation amount (*P*), UVB radiation (*UVB*), air temperature (T_{air}), air pressure (*p*), wind direction (*WD*) and speed (*WS*) (panel *a*) and concurrent 2-min mean lake temperatures at depths from 0.2 to 27 m during the time period from 6 July, 2019 at 00:00 LST to 4 November, 2019 at 00:00 LST (panel *b*).

the lowest recorded temperature at a depth of 27 m was 7.68 °C. This occurrence of "warm" water at greater depths in Prošće Lake was already noticed by Gavazzi (1919), who attributed these temperatures to the influence of a Matica River tributary. Sporadic measurements of water temperatures of the Matica River at various times of a year and for various years show values from 7.0 to 11.3 °C (Petrik, 1961), 10.2 °C (Kempe and Emeis, 1985), and 7.6 ± 0.6 °C (Vurnek et al., 2016). As argued by Gavazzi (1919), this tributary water is rich in suspended matter, and therefore has higher density (and higher turbidity) than the lake water. Thus, it penetrates deep into the lake which results in a temperature increase in the deep lake layers and occasionally, even in the bottom layer. Such
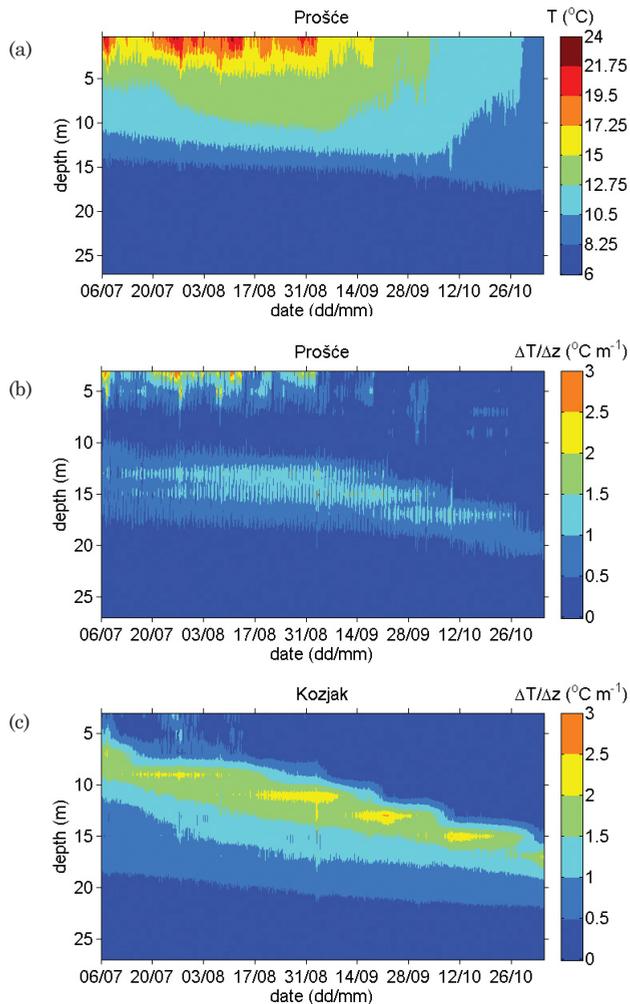
Figure 3. Observed Prošće Lake temperatures (panel *a*) and vertical temperature gradients over depths from 3 to 27 m for the two lakes, Prošće and Kozjak (1st and 12th in the lake chain) during the period from 6 July at 00:00 LST to 4 November 2019 at 00:00 LST (panels *b* and *c*, respectively).

a thermal structure differs from that which was found for the deepest part of the 12th lake in the chain (Kozjak) in which during the period of lake stratification, the observed temperatures of the bottom layers were approximately 4 °C (Klaić et al., 2020).

The difference in thermal structure between the two lakes is further illustrated in Figs. 3b and c. It was observed that the vertical temperature gradients in the metalimnetic region are generally lower for Prošće Lake than for Kozjak Lake. Additionally, throughout nearly the entire stratification period, two regions with comparably elevated values for the vertical temperature gradient were found (Fig 3b). As of mid-July, the maximum $\Delta T / \Delta z$ values in the first thermocline region were found at a depth of approximately 12 m while for the second thermocline region, they were roughly at a depth of 14 m. Such a multilayer structure was seen until the mid-September while after this and for a period of approximately one week, a single thermocline region with maximum values of $\Delta T / \Delta z$ values at a depth of approximately 13 m is seen. From approximately 20 September until 10 October, the most frequently the two thermocline regions are seen again, and the maximum values of $\Delta T / \Delta z$ were at depths of 13 and 16 m, respectively. In contrast to Prošće Lake, during the entire observational period Kozjak Lake had only one thermocline region (Fig. 3c).

As expected, the above multilayer thermal structure in Prošće Lake was accompanied with complex vertical profiles for other lake variables. As one example, in Fig. 4 we show vertical profiles of the lake temperature, water density, vertical temperature gradient, vertical gradient of water density and Brunt-Väisälä frequency for 10 October at 04:00 LST (red lines in Fig. 4). Apart from the multilayer thermal and density structure (panels a and b, respectively), two distinct thermocline/pycnocline regions were found with a maximum $\Delta T / \Delta z$ at depths of approximately 11 and 16 m (panel c) and maximum $\Delta \rho / \Delta z$ at approximately 10 and 16 m, respectively (panel d), and corresponding peaks in hydrostatic stability (high values of N^2) at the same depths (panel e), which are typical for thermocline regions (*e.g.*, Gerkema and Zimmerman, 2008). To summarize, for this particular time (10 October at 04:00 LST) vertical structure of the lake can be approximated with a four-layer model. Specific layers are following: epilimnion (from the lake surface to ≈ 9 m), upper metalimnion (from ≈ 9 m to ≈ 15 m), lower metalimnion (from ≈ 15 m to ≈ 20 m) and hypolimnion (from ≈ 20 m to the lake bottom). In addition, we note that the uppermost part of the lake (specifically, the first 0.5 m and the layer between 3 and 9 m) were at that specific time slightly hydrostatically unstable. This is seen from very small, but negative values of N^2 which points to conditions that are favorable for the vertical mixing of the water.

On the other hand, for 22 September at 00:00 LST (black lines in Fig. 4), only one prominent thermocline/pycnocline region was found at a depth of approximately 14 m. This is seen from the vertical profiles of $\Delta T / \Delta z$, $\Delta \rho / \Delta z$ and N^2 (panels c–e) which all have maximum values at this particular depth. We also note that these maximum values are noticeably higher than those observed for 10 October at 04:00 (red lines in Figs. 4c-e) and 30 September (blue lines in Figs. 4c-e). Thus, we conclude that for this particular time the lake stratification can be approximated with a two-layer model, where epilimnion and hypolimnion stretch from the lake surface to ≈ 14 m and from ≈ 14 m to the lake bottom.

Finally, for 30 September at 12:00 LST (blue lines in Fig. 4) the depth of epilimnion is rather low (≈ 5 m). Conversely, metalimnetic region is deep, and it stretches from ≈ 5 to ≈ 20 m. Although in this region four sublayers are seen (specifically, first layer from ≈ 5 to ≈ 9 m, second from ≈ 9 to ≈ 13 m, third from ≈ 13 to ≈ 17 m, and the fourth from ≈ 17 to
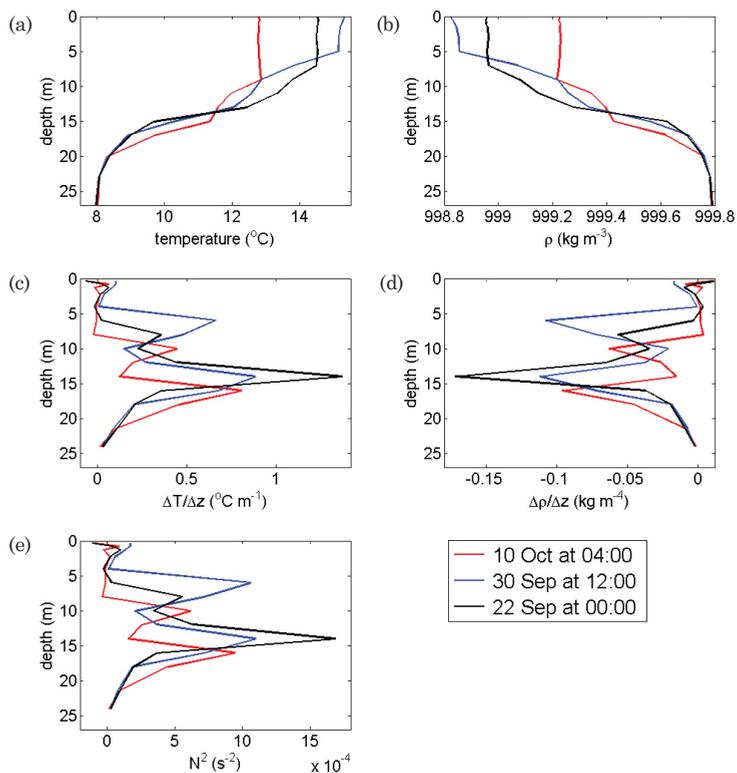
Figure 4. Vertical profiles of lake temperature, water density (ρ), vertical temperature gradient ($\Delta T / \Delta z$), vertical gradient of water density ($\Delta \rho / \Delta z$) and Brunt-Väisälä frequency squared (N^2) at measuring point P1 for 22 September at 00:00 LST, 30 September at 12:00 LST and 10 October at 04:00 LST. Position of point P1 is depicted in Fig. 1.

≈ 20 m; blue lines in Figs. 4a and b), vertical profiles of the lake temperature (Fig. 4a) and water density (Fig. 4b) in this region do not departure much from straight lines. Moreover, the hydrostatic stability of the entire layer from ≈ 5 to ≈ 20 m is high (higher than that one observed for 10 October at 04:00 LST), which is seen from the observed values of N^2 (blue line in Fig. 4e). Therefore, we conclude that for this particular time the lake stratification can be approximated with a three-layer model, where epilimnion, metalimnion and hypolimnion are found at the depths from the lake surface to ≈ 5 m, from ≈ 5 m to ≈ 20 m, and from ≈ 20 m to the lake depth, respectively.

Figures 5–7 show the PSDs for atmospheric variables and lake temperatures that were measured at points M and P1 (Fig. 1) during the observational period (6 July–4 November, 2019), respectively. PSDs were calculated from hourly mean values as described in Section 3. As expected, the atmospheric variables exhibited evident diurnal periodicity and showed the presence of both 1st and higher order harmonics of the 24 h period (Fig. 5). As seen from Fig. 6, apart from the very low frequencies (≈ 0 cph), the frequency (hereafter, ν) that contained the most energy was $\nu = 0.0417$ cph. (This fre-
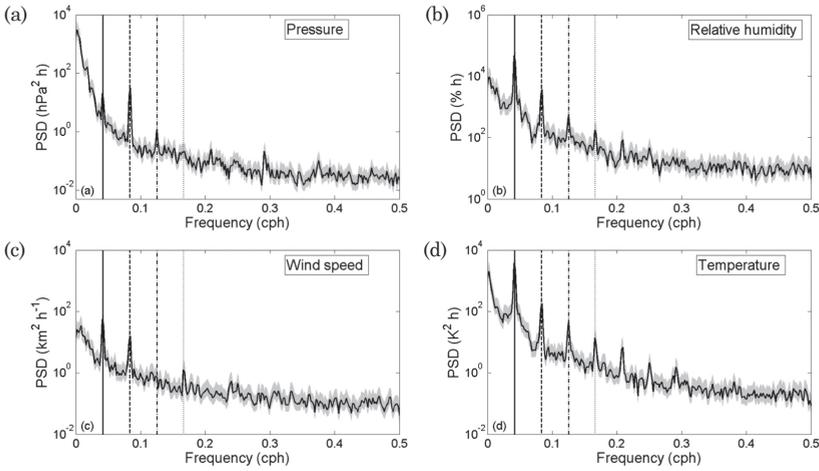
Figure 5. Power spectral densities (PSD, full black lines) for meteorological variables: air pressure (*a*), relative atmospheric humidity (*b*), wind speed (*c*), and air temperature (*d*). PSDs were computed from the hourly mean values measured at point M (Fig. 1) from 6 July to 4 Novem-ber, 2019, as described in Section 3. Shaded gray areas show 95% confidence intervals. Full, dashed, dash-dotted, and dotted vertical lines correspond to periods of 24.0, 12.0, 8 and 6.0 h.

quency, which corresponds to the first harmonic of the 24.0 h period, emerged as the lake response to diurnal atmospheric forcing.) Specifically, pronounced peaks in the PSD at orders of magnitude from 10^0 to 10^1 were found for $v = 0.0417$ cph in the upper 7 m of the lake (approximately) and at depths between 11 and 17 m. We note that the latter depths coincided with the positions of the two thermocline regions shown in Fig. 3b. Furthermore, at the same depths, a tongue of elevated energy magnitudes from 10^{-1} to 10^0 that stretched from $v = 0.0417$ cph (*i.e.*, period of 24.0 h) toward $v > 0.2$ cph (that is, toward periods below 5 h) was present.
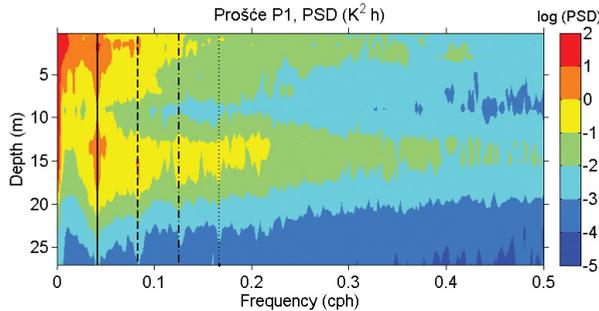
Figure 6. Vertical profile of power spectral density (PSD) over lake depths from 0.2 to 27 m. PSDs were calculated from the hourly mean lake temperatures measured at point P1 (Fig. 1) from 6 July, 2019 to 4 November, 2019, as described in Section 3. The vertical solid, dashed, dash-dotted, and dotted lines correspond to periods of 24.0, 12.0, 8.0, and 6.0 h, respectively.
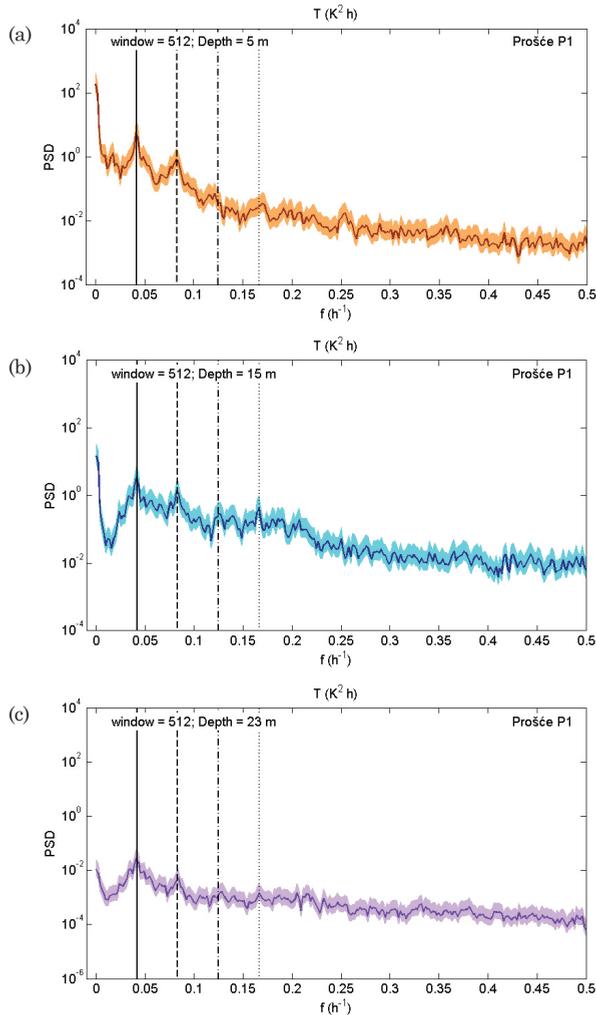
Figure 7. Power spectral densities (PSDs) for lake temperatures at 5, 15 and 23 m (panels *a*, *b* and *c*, respectively). Each of these depths is located in a different lake layer, namely, in the epilimnion (*a*), metalimnion (*b*) and hypolimnion (*c*). PSDs were calculated from the hourly mean temperatures measured at point P1during 6 July–4 November 2019. The solid lines and shaded areas depict PSDs and 95% confidence intervals, respectively. The vertical solid, dashed, dash-dotted, and dotted lines correspond to periods of 24.0, 12.0, 8.0, and 6.0 h, respectively.

Figure 7 shows the individual spectra for only one depth per distinct lake layer, *i.e.*, for one point in the epilimnion (5 m, panel a); metalimnion (15 m, panel b); and hypolimnion (23 m, panel c), respectively. However, detailed inspection of the spectra for all fifteen individual depths (not shown here) showed prominent peaks in the PSDs for a diurnal period ($v = 0.0417$ cph) throughout the entire layer

from 0.2 to 23 m. Apart from depths 1.5–3 m and 13–17 m, where the PSD values for a 24.0 h period were higher than those found for shallower depths, the PSD peaks generally decreased downward from $2.7 \cdot 10^1$ K^2h at a depth of 0.2 m to $2.8 \cdot 10^{-2}$ K^2h at a depth of 23 m.

Higher order harmonics, which are generally produced by interaction of a fundamental wave (here, a wave with diurnal periodicity) with a nonlinear medium (Scott, 2005), were found at most inspected depths. Some of these can be seen in Fig. 7. Specifically, the 2nd harmonic (that corresponds to a period of 12.0 h) was found at all three shown depths, the 3rd harmonic (period of 8.0 h) was seen at a depth of 15 m while the 4th harmonic (period of 6.0 h) was found at 15 and 23 m. Furthermore, at individual depths, the peak PSD values decreased with the order of the harmonics except for a depth of 15 m (Fig. 7b) at which the PSD value for the 4th harmonic ($4.5 \cdot 10^{-1}$ K^2h) was approximately 50% higher than the value for the 3rd harmonics ($2.9 \cdot 10^{-1}$ K^2h). Since the depth of 15 m was in the region of high vertical temperature gradients (Fig. 3b), we assumed that the observed energy peak for the 6.0 h period was a result of both a 4th harmonic that was produced by diurnal atmospheric forcing of the lake and an internal seiche with the same (or similar) period.

To verify the above assumption, we inspected the time interval that was characterized by along-basin winds which generally may produce internal seiches. As seen in Fig. 2a, as of approximately 20 September until the end of the observational period, the winds were mainly in the along-basin direction, *i.e.*, southern (directions close to 180 deg) or northern (directions close to 0 or to 360 deg) and wind speeds were frequently stronger than they were at other times. Therefore, we selected the time interval from 22 September at 00:00 to 22 October at 00:00. (Regrettably, we did not include the last episode of steady, quite strong southern winds from 28 October to 4 November since it was at the end of the observational period; thus, information on the later lake response was not available.) As seen in Fig. 2b, during the selected time interval, the amplitudes of lake temperature oscillations at a depth of 15 m were generally greater than those at other times. Similar increases in lake temperature amplitudes were also found at a depth of 17 m. The observed winds and lake temperatures during the selected time interval are shown in Fig. 8. It was observed that during this time interval, wind speeds were mainly greather than the average value, WS_{avg}, that was obtained for the entire observational period ($WS_{avg} = 1.25$ ms^{-1}). Furthermore, the higher wind speeds were mainly associated with southern winds (directions ≈ 180 deg). Typically, stronger inland winds from these directions point to a synoptic setup which is associated with sirocco flow over the Adriatic that frequently produces various oscillatory responses in the sea (*e.g.*, Vilibić et al., 2004; Bertotti et al., 2011; Dutour Sikirić et al., 2018). Occasionally, during the selected time interval, north-northwestern winds (≈ 330 deg, roughly along-basin) were also accompanied by higher wind speeds (Figs. 8 a and b). These flows point to synoptic forcing associated with bora over the Adriatic and consequent sea response (*e.g.*, Orlić et al, 1994; Bergamasco and Gačić, 1996; Vilibić and Supić, 2005). Apart from the oscillations of the lake temperature at 15 and 17 m, Fig. 8 also shows occasional prominent temperature jumps (even up to ≈ 2 °C) at depths of 5 and 7 m while the oscillations at other depths were substantially weaker. A closer view of several such events is shown in Fig. 9.

As seen in the top of Fig. 9, the temperatures at depths of 5 and 7 m and at depths of 15 and 17 m oscillate against each other. This points to the presence of a second vertical, first horizontal (V2H1) seiche mode. Additionally, Fig. 9 (bottom) shows vertical
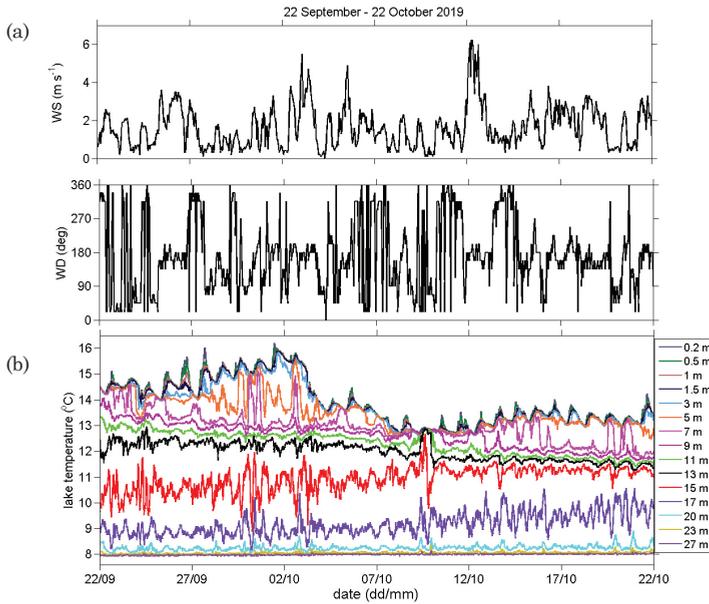
Figure 8. Wind speeds (WS) and directions (WD) (panel *a*) and lake temperatures (panel *b*) during the selected time interval from 22 September at 00:00 to 22 October at 00:00.
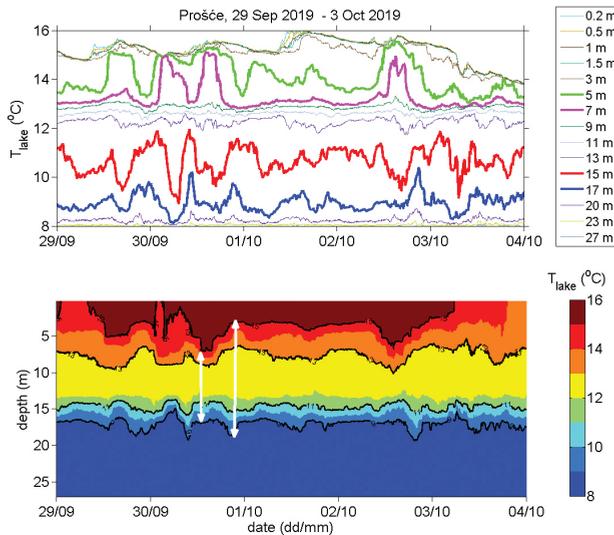
Figure 9. A closer view of those events with prominent lake temperature oscillations at depths of 5, 7, 15 and 17 m (*top*) and a concurrent vertical profile of the lake temperatures (*bottom*). White double arrows show the metalimnion thickness at two specific times. Black lines at bottom panel show isotherms of 9, 11, 13 and 15°C, respectively.

squeezing and stretching of the deep metalimnion which generated the second vertical mode (*e.g.*, Münnich et al., 1992). We note that higher vertical modes were not observed for nearby Kozjak Lake (Klaić et al., 2020), which is a somewhat larger and deeper lake of comparable size but with more complex bathymetry and an inlet that is approximately 1.2 km distant from the Prošće outlet (although the path of water flow between the two lakes is somewhat longer).

Figure 10 shows the PSDs for lake temperatures, air pressures and the wind speeds corresponding to the time interval (22 September–21 October) which was associated with stronger along-basin winds while the observed PSD peaks are listed in Tab. 1. As seen from Fig. 10a at the depth of 15 m and followed by 17, 7 and 5 m stood out with respect to the energy content while the energy levels associated with other depths were generally weaker. Furthermore, while diurnal periodicity in air pressure and wind speed fields was present during the entire observational period (Figs. 5 a and c), the same was not observed for the selected time interval with stronger along-basin winds (Figs. 10 b and c and Tab. 1). This is not surprising since the stronger winds are caused by synoptic disturbances which do not exhibit diurnal periodicity.

As seen in Tab. 1, the majority of periods seen for lake temperatures are the same as the periods seen for the air pressure and/or wind speed. In other words, these periods corresponded to the forced lake temperature oscillations that were caused by periodic atmospheric forcing of the lake surface. Exceptions were the periods of 5.12 h (found for a depth of 5 m); 6.09 h (found for all four depths, namely, 5, 7, 15 and 17 m); and 7.11 h (at a depth of 15 m). These periods were clearly associated with free baroclinic oscillations since they were independent of external forcing. Instead, they were basin-dependent (*e.g.*, Rabinovich, 2009).

The highest energies that were associated with lake temperatures at particular depths corresponded to a period of 25.60 h and were observed at all four depths where they had an order of magnitude of 10^1. These were followed by energies corresponding to a period of 11.64 h with the energy at 15 m being the greatest. In comparison with the energies observed for the forced oscillations (*i.e.*, for periods of 25.60 and 11.64 h), the energies associated with free baroclinic oscillations (*i.e.*, periods of 7.11, 6.09 and 5.12 h shown in Tab. 1) were 1–2 orders of magnitude lower, where the highest among them (0.58 K^2h) was found for a depth of 15 m and period of 6.09 h. This is in accordance with results of previous studies of Alpnacher See, Switzerland (Münnich et al., 1992), Sau reservoir, Spain (Vidal et al., 2005), Bromont Lake, Canada (Pannard et al., 2011) and Iseo Lake, Italy (Valerio et al., 2019) which show that higher vertical modes (*i.e.*, forced baroclinic oscillations) dominate over the V1H1 mode (*i.e.*, free baroclinic oscillations). The authors of these studies argue that the forced, higher vertical modes are more energetic due to the resonance between the periodic wind forcing and waves. On the contrary, for Bala Lake (Llyn Tegid), UK (Simpson et al., 2011) such behavior was not observed. Specifically, V1H1 mode was dominant, while V2H1 mode was significant only at times.

Most of the energy for both meteorological variables was associated with the period of 128 h (≈ 5.3 days). This period was found for lake temperature at 7 m and for air pressure and wind speed and may be associated with cyclonic activity. Namely, studies of several different regions in Croatia have reported occurrences of cyclonic weather every 2.8 days (Adriatic region, analysis of four September–November seasons, Horvath et al., 2008); 8.3 days (inland Croatia, analysis of 30 fall seasons, Lončar and Bajić, 1994); and
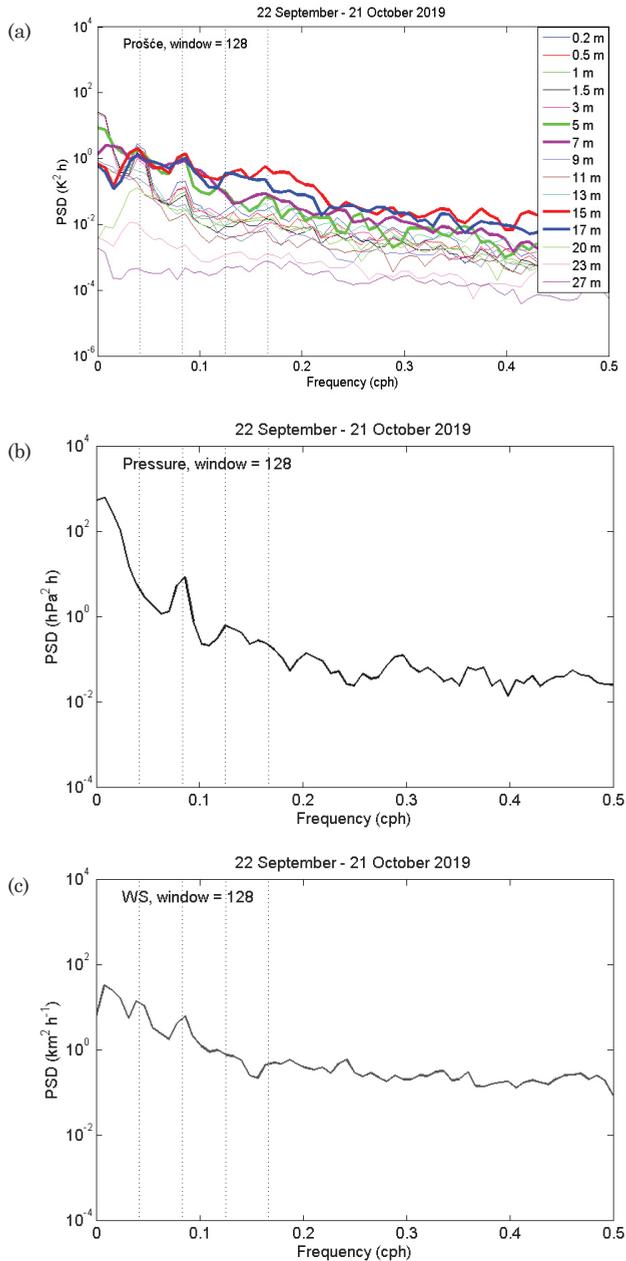
Figure 10. Power spectral densities (PSDs) for lake temperatures at depths from 0.2 to 27 m (*a*), air pressures (*b*), and wind speeds (*c*) observed during the time interval from 22 September at 00:00 to 22 October at 00:00. PSDs were calculated as described in Section 3. Four vertical dotted lines correspond to periods of 24.0, 12.0, 8.0 and 6.0 h.

Table 1. Observed PSD peaks and corresponding periods found for the lake temperatures (T_{lake}) at 5, 7, 15, and 17 m and for air pressure (p) and wind speed (WS) measured during the selected time interval that was associated with stronger, along-basin winds (i.e., 22 September – 21 October, 2019). Those periods that were observed solely for lake temperatures are shown in bold.

Period (h)	T_{lake}				p	WS
	5 m (K²h)	7 m (K²h)	15 m (K²h)	17 m (K²h)	(hPa²h)	(km²h⁻¹)
128 (≈ 5.3 days)		2.49			649.00	33.74
25.60	1.82	1.19	2.00	1.32		14.45
11.64	0.94	0.08	1.41	1.02	8.61	6.26
8.50	0.13					1.02
8.00				0.36	0.62	
7.11			**0.47**			
6.09	**0.07**	**0.09**	**0.58**	**0.22**		
5.33			0.37	0.11		0.60
5.12	**0.03**					
4.92					0.14	
4.12			0.05			0.61
3.88	0.02				0.05	
3.36					0.13	

8.9 days (Zagreb, analysis of 2 year data segment, Klaić, 2001). Higher energies were also found for the wind speed for a 25.60 h period, and for both the wind speed and air pressure for a period of 11.64 h.

Figure 11 shows the magnitude-squared coherence (γ^2) values between the lake temperatures at each depth and the lake temperatures at 15 m for the time interval with stronger along-basin winds. The corresponding cross-spectrum phases are also depicted. Depth of 15 m was selected since it exhibited the highest energy content (Fig 10a).

Between the two prominent periods of forced oscillations that were found for the lake depths listed in Tab. 1, the period of 25.60 h was associated with higher PSD values at all four depths. For this period, γ^2 is the highest (from 0.6 to 1) for depths between 11 and 23 m (Fig. 11a) and was followed by depths between 5 and 7 m (γ^2 between 0.4 and 0.6). Corresponding cross-spectra phases (Fig. 11b) show that in the lake column between 5 and 23 m, the phase lag changed from ≈ 150 deg at the top of the column (red area) to over ≈ −180 deg (depths from 9 to 13 m, blue area) and to ≈ 150 deg at the column bottom (red) which suggested the presence of a V3H1 mode. Moreover, the presence of three vertical modes implied the existence of four-layer lake structure. We note that such a structure was present in the vertical profiles shown with red lines in Fig. 4.

The second period of forced lake temperature oscillations (11.64 h) was accompanied with elevated γ^2 values of comparable magnitudes (from 0.8 to 1) at depths from 5 to 7 and from 15 to 17 m, respectively (panel a). However, cross-spectrum phases exhibited a shift between the upper and lower lake depths of ≈ 180 deg (panel b) which pointed to a V2H1 mode.
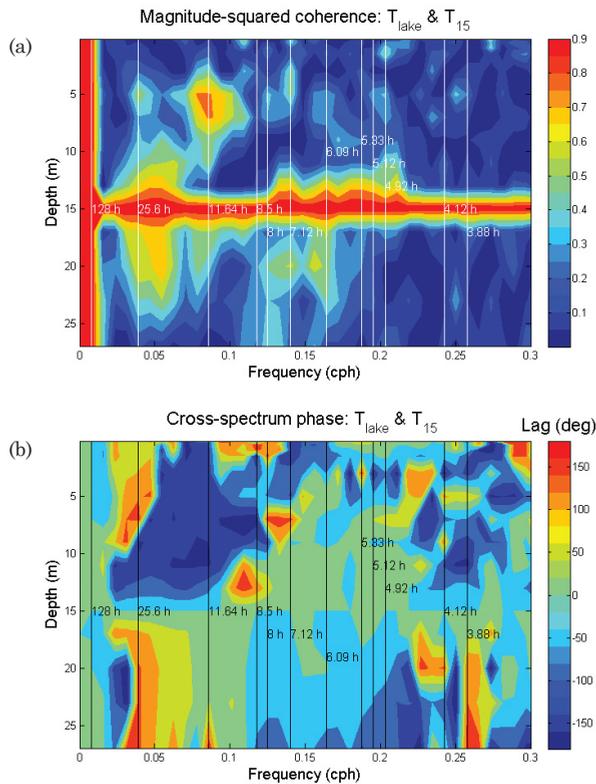
Figure 11. Magnitude-squared coherence (γ^2) values between lake temperatures at each depth and lake temperatures at 15 m (panel *a*) for the time interval with stronger along-basin airflow (22 September–21 October 2019). Panel *b* shows the corresponding cross-spectrum phases. Solid black vertical lines correspond to the periods listed in Tab. 1.

Considering free baroclinic lake temperature oscillations, a period of 6.09 h was most prominent since it was associated with both the highest PSD values and it was found for all four lake depths (Tab. 1). As seen in Fig. 11b, the cross-spectrum phase was mainly close to 0 throughout entire lake column from 5 to 17 m (at some depths, somewhat higher values are found but their absolute values do not exceed 30 deg). Thus, we conclude that this period corresponded to V1H1 mode.

Finally, we calculated theoretical periods for two different lake stratifications presented in Fig. 4. As already argued above, the first (22 September at 00:00 LST; black lines in Fig. 4) and the second stratification case (30 September at 12:00 LST; blue lines in Fig. 4) can be approximated with a two- (Eq. 3) and a three-layer model (Eq. 4), respectively. Results are summarized in Tab. 2. It is seen that periods calculated for these two particular cases are noticeably lower than those observed for the entire time interval associated with along-basin winds (*i.e.*, 22 September–21 October). As already pointed by other authors (*e.g.*, Fricker and Nepf, 2000), more accurate modeling of internal seiches would require the use of more realistic density profiles and basin shape.

Table 2. Theoretical periods of obtained for two different lake stratifications, assuming an idealized rectangular basin with L = 2,000 m and h = 27 m and homogenous lake layers. Note that observed periods correspond to the entire time interval from 22 September–21 October 2019.

Date Time	Theoretical model Mode / Equation	Layer depths and densities	Period (h) Theoretical / Observed
22 September 00:00 LST	two-layer V1H1 / Eq. 3	$h_E = 14$ m $h_H = 13$ m $\rho_E = 999.09$ kg m^{-3} $\rho_H = 999.76$ kg m^{-3}	5.28 / 6.09
30 September 12:00 LST	three-layer V2H1 / Eq. 4	$h_E = 5$ m $h_M = 15$ m $h_H = 7$ m $\rho_E = 998.85$ kg m^{-3} $\rho_M = 999.38$ kg m^{-3} $\rho_H = 999.78$ kg m^{-3}	9.10 / 11.64

5. Conclusions

An investigation of the oscillations in lake temperatures that were observed for Prošće, Plitvice Lakes, Croatia revealed a complex response of the lake interior to atmospheric forcing. Apart from the V1H1 mode of an internal seiche, which is most commonly observed in lakes, our results suggest that higher vertical baroclinic modes, V2H1 and V3H1, of the internal seiche were also excited. We believe that three prominent periods that were observed for the time interval associated with stronger along-basin winds correspond to V1H1 (period of 6.09 h), V2H1 (period of 11.64 h), and V3H1 (period of 25.60 h). While the V1H1 mode represents free baroclinic internal oscillations, the V2H1 and V3H1 modes corresponded to forced baroclinic internal oscillations (*i.e.*, the same periodicity was found in the atmospheric fields) for which the latter two were associated with the existence of three and four lake layers, respectively. Among these three prominent modes, V3H1 and V1H1 exhibited the highest and the lowest energy content, respectively. The fact that forced oscillations were more energetic than free oscillations is in accordance with previous lake studies pointing to the role of resonant response of higher vertical modes to periodic wind forcing.

Such complex seiching was not reported in a previous study of the nearby, somewhat larger Kozjak Lake (for both lakes, the effects of the Coriolis force can be neglected) which belongs to the same cascade lake system and is thus also fed by water that originated from Prošće Lake and has more complex bathymetry. For Kozjak Lake, only the V1H1 mode was reported (however, these results were obtained for a different observational period). We believe that the differences between the two lakes may exist due to the influence of tributary water (*i.e.*, Matica River) which feeds Prošće Lake. Specifically, due to denser tributary water, Prošće Lake did not attain the typical stratification that is characterized by hypolimnetic temperatures close to 4 °C (which was established in Kozjak Lake). Instead, the hypolimnetic temperatures were always above 7.6 °C. This, in comparison with Kozjak Lake resulted in weaker thermal stratification; consequently, there were weaker vertical gradients in water density, a thicker metalimnion (both, the absolute metalimnion thickness and the thickness relative to the maximum lake depth were higher for Prošće Lake) and even the presence of two metalimnetic layers. Since metalimnions which are thick enough with respect to the entire lake depth and/or multiple metalim-

netic layers are prerequisites for excitation of higher vertical modes (*e.g.*, Münnich et al, 1992; Vidal et al., 2005; Pannard et al., 2011), we conclude that for Prošće Lake, this condition was fulfilled due to the influence of tributary water. However, to reach further conclusions regarding the differences in seiching between the two lakes, spectral analysis of lake temperatures for Kozjak Lake for the same observational period as that used in the present study should be performed.

Additionally, Prošće Lake is ≈ 100 m higher in altitude and is in less-sheltered position than Kozjak Lake. Thus, it is very likely that it is exposed to stronger winds than Kozjak Lake. This might also contribute to different response of the two lakes to atmospheric forcing.

Results of the two- and three-layer idealized models (Eqs. 3 and 4), where a rectangular basin with constant depth is assumed, suggest periods of V1H1 and V2H1 modes that are noticeably smaller than the observed. Therefore, a modeling study of internal seiches in Prošće Lake that is based on more complex, Eulerian hydrodynamic lake model (that is, more realistic both lake bathimetry and vertical profiles of water density), would be desirable.

References

Babinka, S. (2007): Multi-tracer study of karst waters and lake sediments in Croatia and Bosnia-Herzegovina: Plitvice Lakes National Park and Bihać Area. PhD Dissertation, Rheinischen Friedrich-Wilhelms-Universität Bonn, Germany, 167 pp.

Bergamasco, A. and Gačić, M. (1996): Baroclinic response of the Adriatic Sea to an episode of bora wind, *J. Phys. Oceanogr.*, **26**, 1354–1368. https://doi.org/10.1175/1520-0485(1996)026<1354:BROTAS>2.0.CO;2.

Bertotti, L., Canestrelli, P., Cavaleri, L. and Zampato, L. (2011): The Henetus wave forecast system in the Adriatic Sea, *Nat. Hazards Earth Syst. Sci.*, **11**, 2965–2979, https://doi.org/10.5194/nhess-11-2965-2011.

Boegman, L. (2009): Currents in stratified water bodies 2: Internal waves. In: G. E. Likens (Ed.), *Encyclopedia of inland waters*, *Vol.* 1, Oxford, Elsevier, 539 – 558.

Dutour Sikirić, M., Ivanković, D., Roland, A., Ivatek-Šahdan, S. and Tudor, M. (2018): Operational wave modelling in the Adriatic Sea with the Wind Wave Model, *Pure Appl. Geophys.*, **175,** 3801–3815, https://doi.org/10.1007/s00024-018-1954-2.

Fricker, P. D. and Nepf, H. M. (2000): Bathymetry, stratification, and internal seiche structure, *J. Geophys. Res.*, **105**, 14,237–14,251, https://doi.org/10.1029/2000JC900060.

Gavazzi, A. (1919): *Prilozi za limnologiju Plitvica, Prirodoslovna istraživanja Hrvatske i Slavonije.* JAZU, 14, 3–37 (in Croatian).

Gerkema, T. and Zimmerman, J. T. F. (2008): *An introduction to internal waves.* Lecture notes, Royal NIOZ, Texel, 207 pp.

Golubić (1966): Vergleichende Untersuchungen des Lichtklimasin den Plitvizer Seen, *Verh. Internat. Verein. Limnol.*, **16**, 107–110, https://doi.org/10.1080/03680770.1965.11895670.

Heaps, N. S. (1961): Seiches in a narrow lake, uniformly stratified in three layers, *Geophys. J. Int.*, **5**, 134–156, https://doi.org/10.1111/j.1365-246X.1961.tb00418.x.

Horvath, K., Lin, Y.-L. and Ivančan-Picek, B. (2008): Classification of cyclone tracks over the Apennines and the Adriatic Sea, *Mon. Wea. Rev.*, **136**, 2210–2227, https://doi.org/10.1175/2007M-WR2231.1.

Horvatinčić, N., Sironić, A., Barešić, J., Sondi, I., Krajcar Bronić, I. and Borković, D. (2018): Mineralogical, organic and isotopic composition as palaeoenvironmental records in the lake sediments of two lakes, the Plitvice Lakes, Croatia, *Quat. Int.*, **494**, 300–313, https://doi.org/10.1016/j.quaint.2017.01.022.

Hutter, K., Wang, Y. and Chubarenko, I. P. (2011): Higher-order baroclinicity (II)interpretation of lake data with rotating and non-rotating models. In: *Physics of lakes. Advances in geophysical and environmental mechanics and mathematics, Vol. 2*, Springer-Verlag, Berlin, 251–286, https://doi.org/10.1007/978-3-642-19112-1_16.

Kempe, S. and Emeis, K. (1985): Carbonate chemistry and the formation of Plitvice Lakes, in *Transport of Carbon and Minerals in Major World Rivers*, *Pt.* 3, edited by Degens, E. T., Kempe, S. and Herrera, R., Mitt. Geol.-Paläont. Inst. Univ. Hamburg, SCOPE/UNEP Sonderband, **58**, 351–383.

Klaić, Z. B. (2001): Weather types and traffic accidents, *Coll. Antropol.*, **25**, 245–254.

Klaić, Z. B., Rubinić, J. and Kapelj, S. (2018): Review of research on Plitvice Lakes, Croatia in the fields of meteorology, climatology, hydrology, hydrogeochemistry and physical limnology, *Geofizika*, **35**, 189–278, https://doi.org/10.15233/gfz.2018.35.9.

Klaić, Z. B., Babić, K. and Orlić, M. (2020): Evolution and dynamics of the vertical temperature profile in an oligotrophic lake, *Hydrol. Earth Syst. Sci.*, **24,** 3399–3416, https://doi.org/10.5194/hess-24-3399-2020.

Lončar, E. and Bajić, A. (1994): Tipovi vremena u Hrvatskoj, *Hrv. met. čas.*, **29**, 31–41 (in Croatian).

Mortimer, C. H. (1953): The resonant response of stratified lakes to wind, *Schweiz. Z. Hydrol.*, **15**, 94–151.

Münnich, M., Wüest, A. and Imboden, D. M. (1992): Observations of the second vertical mode of the internal seiche in an alpine lake, *Limnol. Oceanogr.*, **37**, 1705–1719. https://doi.org/10.4319/lo.1992.37.8.1705.

Orlić, M., Kuzmić, M. and Pasarić, Z. (1994): Response of the Adriatic Sea to the bora and sirocco forcing*, Cont. Shelf Res.*, **14**, 91–116, https://doi.org/10.1016/0278-4343(94)90007-8.

Pannard, A., Beisner, B. E., Bird, D. F., Braun, J. and Planas, D. (2011): Recurrent internal waves in a small lake: Potential ecological consequences for metalimnetic phytoplankton populations, *Limnol. Oceanogr. Fluids Environ.*, **1**, 91–109, https://doi.org/10.1215/21573698-1303296.

Pasarić, M. and Slaviček, L. (2016): Seiches in the Plitvice Lakes, *Geofizika*, **33**, 35–52, https://doi.org/0.15233/gfz.2016.33.6.

Patel, R., Kumar, M., Jaiswal, A. K. and Saxena, R. (2013): Design technique of bandpass FIR filter using various window functions, *IOSR-JECE*, **6**, 52–57.

Paul, L. (1987): Influence of seiche-generated light field fluctuations on phytoplankton growth, *Int. Rev. gesamten Hydrobiol.*, **72**, 269-281, https://doi.org/10.1002/iroh.19870720302.

Petrik, M. (1961): Temperatura i kisik Plitvičkih jezera. *Rasprave odjela za matematičke, fizičke i tehničke nauke, JAZU*, **Svezak 11**, 81–119 (in Croatian).

Rabinovich, A. B. (2009): Seiches and harbor oscillations, Chapter 9, *Handbook of Coastal and Ocean Engineering* (Kim, Y.C., Ed), World Scientific Publ., Singapoure, 193–236, http://doi.org/10.1142/9789812819307_0009.

Scott, A. (2005): *Encyclopedia of nonlinear Science*, Routledge, Taylor & Francis Group, New York, 394–396. 33

Simpson, J. H., Wiles, P. J. and Lincoln, B. J. (2011): Internal seiche modes and bottom boundary-layer dissipation in a temperate lake from acoustic measurements, *Limnol. Oceangor.*, **56**, 1893–1906, https://doi.org/10.4319/lo.2011.56.5.1893.

Sun, S., Yan, J., Xia, N. and Sun, C. (2007): Development of a model for water and heat exchange between the atmosphere and a water body, *Adv. Atmos. Sci.*, **24**, 927–938, https://doi.org/10.1007/s00376-007-0927-7.

Valerio, G., Pilotti, M., Lau, M. P. and Hupfer, M. (2019): Oxycline oscillations induced by internal waves in deep Lake Iseo, *Hydrol. Earth Syst. Sci.*, **23**, 1763–1777, https://doi.org/10.5194/hess-23-1763-2019.

Vidal, J., Casamitjana, X, Colomer, J. and Serra, T. (2005): The internal wave field in Sau reservoir: Observation and modeling of a third vertical mode, *Limnol. Oceanogr.*, **50**, 1326–1333, https://doi.org/10.4319/lo.2005.50.4.1326.

Vidal, J., Rueda, F. J. and Casamitjana, X., (2007): The seasonal evolution of high vertical–mode internal waves in a deep reservoir, *Limnol. Oceanogr.,* **52**, 2656–2667, https://doi.org/10.4319/lo.2007.52.6.2656.

Vidal, J. and Casamitjana, X., (2008): Forced resonant oscillations as a response to periodic winds in a stratified reservoir, *J. Hydraul. Eng.-ASCE*, **134**, 416–425, https://doi.org/10.1061/(ASCE)0733-9429(2008)134:4(416).

Vilibić, I., Dadić, V. and Mihanović, H. (2004): Large-amplitude internal Kelvin waves trapped off Split (Middle Adriatic Sea), *Estuar. Coast. Shelf Sci.*, **61**, 623–630, https://doi.org/10.1016/j.ecss.2004.07.003.

Vilibić, I. and Supić, N. (2005): Dense water generation on a shelf: the case of the Adriatic Sea, *Ocean Dyn.*, **55**, 403–415, https://doi.org/10.1007/s10236-005-0030-5.

Vurnek, M., Brozinčević, A., Briški, F. and Matoničkin Kepčija, R. (2016): Distributional patterns of fecal indicator bacteria in spring area of Plitvice Lakes National park, *Period. Biol.*, **118**, 37–44, https://doi.org/10.18054/pb.2016.118.1.2849.

Watson, E. R. (1904): Movements of the waters of Loch Ness, as indicated by temperature observations, *Geogr. J.*, **24**, 430–437.

Welch, P. D. (1967): The use of Fast Fourier Transform for the estimation of power spectra: a method based on time averaging over short, modified periodograms, *IEEE Trans. Audio Electroacoust.*, **AU-15**, 70–73, https://doi.org/10.1109/TAU.1967.1161901.

SAŽETAK

Unutarnji stojni valovi u krškom mezotrofnom jezeru (Prošće, Plitvička jezera, Hrvatska)

Zvjezdana B. Klaić, Karmen Babić i Tomislav Mareković

Tijekom 4-mjesečnog razdoblja (od 6. srpnja do 4. studenog 2019.) proveden je eksperiment mjerenja temperature jezera kako bi se ispitala pojava i osobine unutarnjih stojnih valova u Prošćanskom jezeru (Plitvička jezera, Hrvatska). Dvominutni srednjaci temperature mjereni su u jednoj točki jezera na petnaest dubina u rasponu od 0,2 do 27 m. Analiza tih podataka ukazala je na do sada nepoznatu i prilično složenu strukturu unutarnjih stojnih valova u Prošćanskom jezeru. Spektralne gustoće snage (*PSD*) i kva-

drati magnituda koherencije (γ^2) te pripadne kros-spektralne faze koje su izračunate iz srednjih satnih temperature jezera i tlaka zraka te brzina vjetra ukazale su na prisustvo tri vertikalna moda unutarnjih stojnih valova. Prvi mod (V1H1, period od 6,09 h) odgovara slobodnim baroklinim oscilacijama, dok su drugi (V2H1, period od 11,64 h) i treći mod (V3H1, period od 25,60 h) povezani s prisilnim baroklinim oscilacijama unutrašnjosti jezera. Pobuđivanje viših vertikalnih modova pripisano je utjecaju guste vode pritoka. Zbog utjecaja te vode vertikalni temperaturni gradijenti u unutrašnjosti jezera bili su relativno mali te se u skldu s tim formirao jedan debeo metalinij ili dva zasebna metalimnija. U skladu s tim pojavljivali su se modovi V2H1, odnosno V3H1. Nadalje, jezero zbog utjecaja vode pritoka nije postiglo tipičnu stratifikaciju pri kojoj su temperature u hipolimniju ≈ 4 °C. Umjesto toga tijekom cijelog promatranog razdoblja temperature u hipolimniju su neprekidno bile iznad 7.6 °C.

Ključne riječi: koherencija, viši vertikalni modovi, interni stojni valovi, spektralna gustoća snagem V2H1, V3H1

Corresponding author's address: Zvjezdana B. Klaić, Department of Geophysics, Faculty of Science, University of Zagreb, Horvatovac 95, 10000 Zagreb, Croatia; e-mail: zklaic@gfz.hr

Appendix
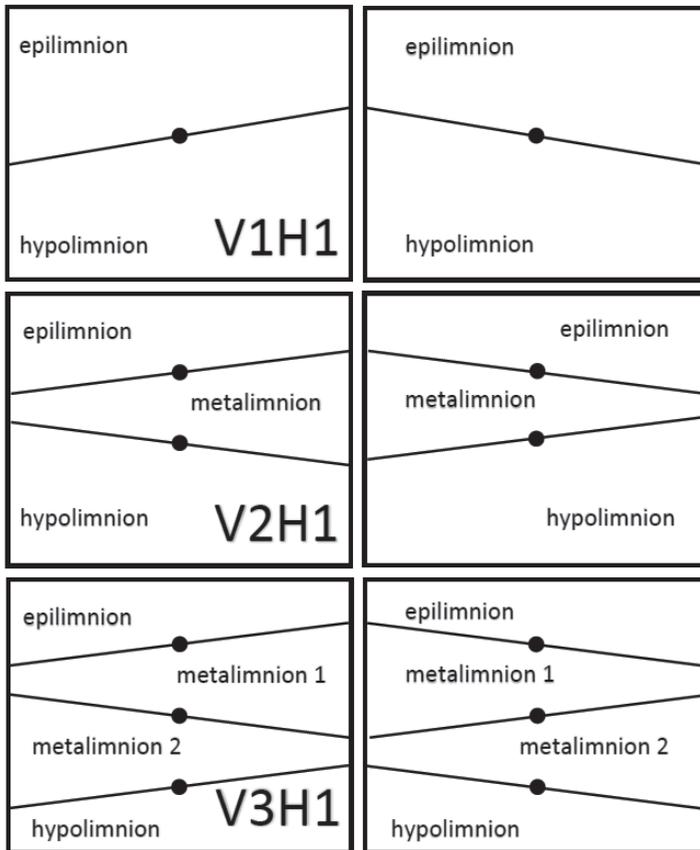
Figure A1. Sketch of internal seiches for V1H1 (*top*), V2H1 (*center*) and V3H1 (*bottom*) modes. Left and right figures show positions of isotherms at the beginning and at the end of an oscillation, respectively. Black full circles show nodal points. While in the horizontal all three modes have only one nodal point, in the vertical V1H1 has one, V2H1 has two, and V3H1 has three nodal points.